International Journal of GEOMATE, Feb., 2026 Vol.30, Issue 138, pp.69-76
ISSN: 2186-2982 (P), 2186-2990 (O), Japan, DOI: https://doi.org/10.21660/2026.138.5283
Geotechnique, Construction Materials and Environment

DEVELOPMENT OF PORE WATER PRESSURE AND DISPLACEMENT IN LIQUEFACTION OF STRATIFIED SAND WITH A CAPPING LAYER

Yelvi[1], *Adrin Tohari[2], Abdul Hakam[3], Jafril Tanjung[4], Handi Sudardja[5], Istiatun[6]

[1,3,4]Civil Engineering Department, Andalas University, Padang, 25163, Indonesia
[2]RC for Geological Disaster, National Research and Innovation Agency (BRIN), Bandung, 40135, Indonesia
[1,5,6]Civil Engineering Department, Politeknik Negeri Jakarta, Depok, 16425, Indonesia

*Corresponding Author, Received: 06 Oct. 2025, Revised: 04 Nov. 2025, Accepted: 09 Nov. 2025

ABSTRACT: The 2018 Palu earthquake (Mw 7.5) caused extensive damage due to liquefaction of saturated sand deposits, even in areas with gentle slopes The presence of a capping layer overlying loose sand deposits is suspected to have exacerbated liquefaction conditions. This study aims to analyze the influence of such a capping layer on excess pore water pressure and lateral displacement in stratified sand. Laboratory tests were conducted using a shaking table. The soil model was prepared in an acrylic box measuring 150×40×50 cm with configurations of dense sand (DS), loose sand (LS), and medium sand (MS). These configurations were tested both with and without a silt capping layer. The shaking table harmonic motion input with an amplitude of 2cm and a frequency of 1.4Hz. The Pore water pressure transducers were installed to monitor the development of pore water pressure ratio (Ru) during dynamic loading. This mechanism is relevant to field liquefaction cases, such as the 2018 Palu event, where a low-permeability layer intensified pore-pressure buildup and prolonged deformation. The results show that the presence of a capping layer significantly affected soil response. Test with a capping layer exhibited faster, higher, and longer-lasting increases in Ru, (persisting for >80 seconds. In addition, lateral displacement in the model with a capping layer was significantly larger (±4.6cm) than in the model without one (<0.89 cm). These findings indicate that a capping layer not only accelerates and prolongs liquefaction by impeding the dissipation of pore water pressure but also amplifies the magnitude of lateral displacement.

Keywords: Liquefaction, Pore Water Pressure, Capping Layer, Stratified Sand, Shaking Table

1. INTRODUCTION

The phenomenon of liquefaction is a critical issue in geotechnical engineering because it can lead to a loss of soil shear strength caused by a sudden increase in pore water pressure. This event generally occurs in saturated sand with uniform gradation and low density when subjected to dynamic loading, particularly during earthquakes [1]. Liquefaction may result in a reduction of soil bearing capacity, lateral displacement, and ultimately the collapse of structures and infrastructure built on such deposits [2].

The 2018 Palu earthquake (Mw 7.5) serves as a real-world example of the devastating impact of liquefaction in Indonesia. The event caused extensive damage in Petobo, Balaroa, and Jono Oge, where massive ground displacement destroyed thousands of homes and claimed numerous lives [3]. Field investigations revealed that, in addition to geological conditions [4,5,6,7] and shallow groundwater levels [8,9,10], the presence of a capping layer was also suspected to influence soil behavior during liquefaction [11,12,13,14,15]. In this study, the capping layer is defined as a low-permeability silt or clay layer overlying liquefiable sand, which restricts drainage during shaking, leading to excess pore-pressure buildup, reduced effective stress and triggering flow-type liquefaction.

Various studies have been conducted to better understand liquefaction mechanisms, including field investigations [16,17,18], numerical analyses [19,20,21], and laboratory experiments [22,23]. One-dimensional (1D) sand column tests have frequently been used to evaluate pore water pressure development [24,25]. However, this method has limitations in representing stratified conditions and lateral ground movement. Shaking table studies provide a more realistic alternative, as they allow for earthquake simulations within stratified soil models [26,27,28,29].

Nevertheless, previous research has been limited in evaluating the fundamental mechanism of water film formation in liquefied sand induced by a capping layer, as studied by Kokusho, T. et al. (2000 and 2025). The influence of the capping layer on soil deformation was not fully analyzed in those studies. Therefore, this research focuses on investigating the effect of a capping layer on the development of the pore water pressure ratio (Ru) in loose sand layers using a 0.16g shaking table. By employing laboratory-scale shaking table experiments, this study aims to provide deeper insights into the liquefaction mechanism in stratified soils under both capped and uncapped conditions.

The principal contribution of this study is the provision of experimental data on the relationship

between the presence of a capping layer and the development of excess pore water pressure, as well as the resulting displacement in stratified sand. The findings of this research may enhance the understanding of liquefaction phenomena and serve as a basis for developing mitigation strategies in earthquake-prone regions of Indonesia.

2. RESEARCH SIGNIFICANCE

This study is of considerable importance in addressing the knowledge gap regarding the role of capping layers in the development of pore water pressure and the potential for flow liquefaction in stratified soils. Previous investigations have generally focused on saturated sand deposits without adequately considering the influence of stratigraphy, thereby limiting the understanding of liquefaction mechanisms. By employing an experimental approach based on shaking table tests, this research is expected to provide scientific contributions in the form of more representative laboratory data that capture the effects of stratified conditions on liquefaction, as well as practical contributions to support disaster mitigation efforts in earthquake-prone regions vulnerable to liquefaction.

3. EXPERIMENTAL METHODOLOGY

This research was conducted in the Soil Testing Laboratory, Department of Civil Engineering at Politeknik Negeri Jakarta, Indonesia, using a laboratory-scale physical model. The experimental method was chosen to replicate field conditions under controlled circumstances, particularly the phenomenon of flow liquefaction in stratified sand with a capping layer. Laboratory testing was carried out using a shaking table capable of generating back-and-forth motion with an amplitude of 2 cm and a frequency of approximately 1.4 Hz, corresponding to the range of ground vibrations that may induce liquefaction in the field.

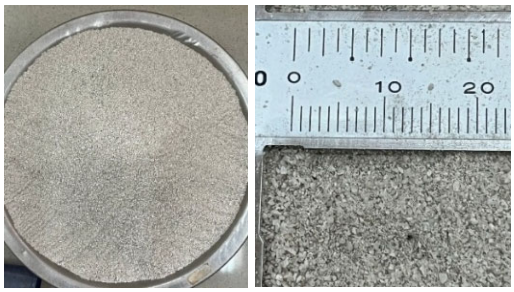

Fig. 1 Clean Sand

3.1 Research Materials

The primary materials used in this study were sand and silt. The sand employed was uniform-graded sand and derived from mineral processing, being relatively free of organic content or clay-sized particles (see Fig. 1).

Based on liquefaction susceptibility criteria from Tsuchida's chart (1970), this sand falls into the category of soils highly vulnerable to liquefaction.

Prior to the shaking table tests, index property tests on the sand and silt were conducted to determine the physical and mechanical characteristics of the soils used in the liquefaction simulations

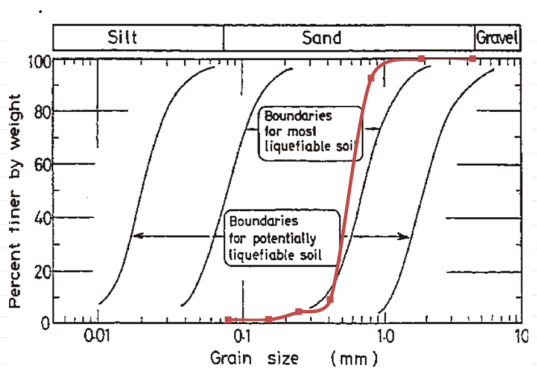

Fig. 2 Sand Gradation on Tsuchida Chart [30]

The physical properties of the sand are presented in Table 1.

Table 1 Index Properties of Sand

Parameter	Symbol	Value	Unit
Specific Gravity	Gs	2.66	-
Maximum Dry Density	γ_{dmax}	1.64	gr/cm^3
Minimum Dry Density	γ_{dmin}	1.37	gr/cm^3
Maximum Void Ratio	e_{max}	0.95	-
Minimum Void Ratio	e_{min}	0.62	-
Coefficient of Uniformity	Cu	1.43	-
Coefficient of Curvature	Cc	0.94	-
D_{50}	D_{50}	0.6	-
Coefficient of Permeability	k	9.52 x 10^{-5}	m/s

In addition to sand, the other material used was silt, which functioned as the capping layer. The silt was obtained from Cikeas, Bogor Regency, and was characterized by a fine texture and low permeability. These properties enabled the silt to act as an impermeable layer above the sand, restricting pore water flow and facilitating the formation of a water film during liquefaction. Thus, the silt was chosen to represent the capping layer conditions observed at the 2018 Palu liquefaction sites. The physical properties of the silt are summarized in Table 2.

3.2 Model Design

The soil model was arranged within a transparent acrylic test box, sized to accommodate both sand and silt layers.

Table 2. Index Properties of Silt

Parameter	Symbol	Value	Unit
Water Content	ω	41.54	%
Unit Weight	γ_m	1.596	gr/cm^3
Specific Gravity	Gs	2.67	-
Liquid Limit	LL	55.964	%
Plastic Limit	PL	31.501	%
Plasticity Index	PI	24.463	%
USCS Classification		MH	-
Coefficient of Permeability	k	5.58x10^{-10}	m/s

The stratification was designed to replicate the soil profile conditions observed at the 2018 Palu liquefaction sites. The thickness of each layer was adjusted according to the 3% slope of the model. The dense sand (DS) layer was approximately 7.4 cm at the upstream side and 3.5 cm at the downstream side. The loose sand (LS) layer was about 15 cm thick, while the medium sand (MS) layer was around 2 cm. A silt capping layer was approximately 1 cm was placed above the MS layer. These dimensions were selected to maintain realistic stratification and to ensure slope stability during shaking.

The Loose Sand (LS) layer was placed as the primary liquefaction zone, underlain by Dense Sand (DS) as a supporting foundation layer, and overlain by Medium Sand (MS). A silt layer was placed above the LS to serve as the capping layer. The model included two variations: with and without the capping layer. The LS and MS layers were inclined at a 3% slope to represent the gentle slopes observed in Palu. The 3% slope used in this model was selected to represent the gentle ground inclinations (approximately 2–5%) observed in the field during the 2018 Palu liquefaction event, as reported by Mason et al. (2019). Pore pressure transducers (PPT) were positioned along the centerline: PPT1 and PPT2 within the LS, and PPT3 at the interface between the LS and MS. Figure 3 illustrates the model without a capping layer, whereas Figure 4 shows the model with a capping layer.

To monitor lateral displacement, one side of the test box was prepared with colored sand layers at 5 cm intervals. Following dynamic loading, the displacement of these colored markers was measured at every 20 cm interval, starting from 5 cm from the left edge of the test box (see Fig. 5).

The displacement of the colored sand markers was measured using an image-based analysis approach. Photographs of the model were taken before and after shaking, and the marker positions were digitized using the PlotDigitizer application. The horizontal and vertical displacements were then quantified by comparing marker coordinates between the pre- and post-test images. This method provided an accurate estimation of lateral movement while minimizing human measurement error

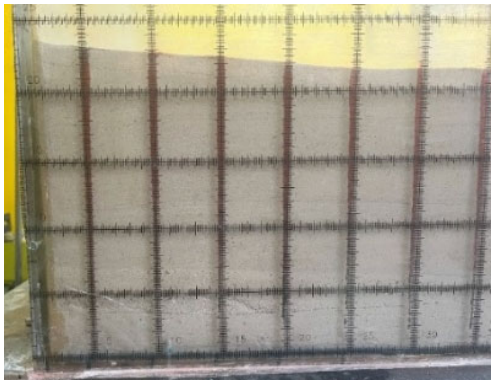

Fig. 5 Colored Sand Applied to the Test Box

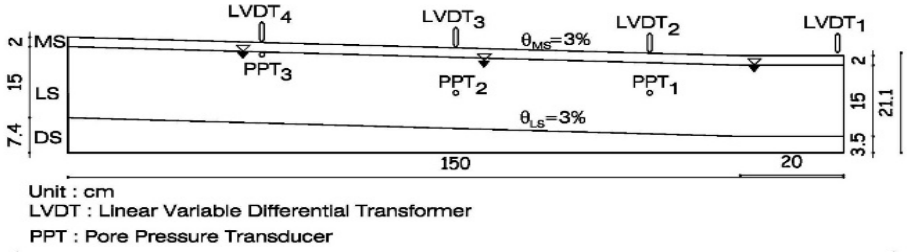

Fig. 3 Model Without Capping Layer

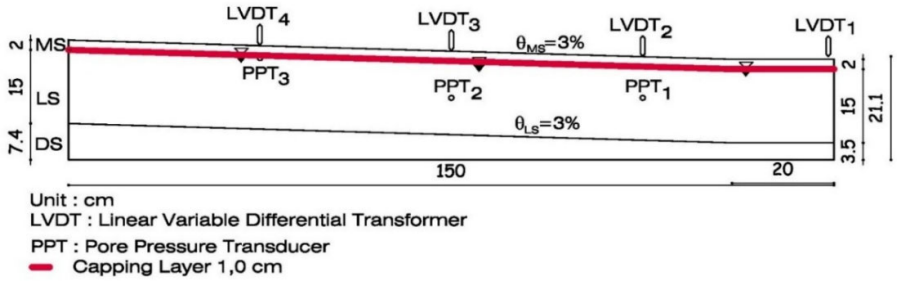

Fig. 4 Model with Capping Layer

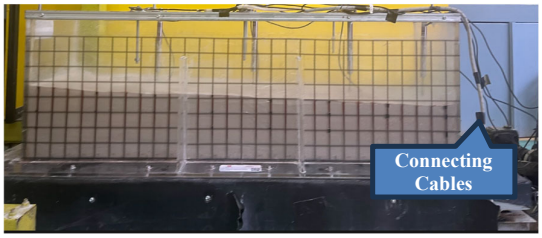

(a)

(b)

Fig. 6 (a) Shaking Table and Acrylic Test Box
(b) Data Acquisition System

3.3 Testing Procedure

Before placement in the test box, the mass of sand was determined according to relative density calculations representing the three compaction states: dense sand (DS), medium sand (MS), and loose sand (LS). The DS layer functioned as a stable foundation in the model, designed to resist vertical movement of the overlying layers during shaking, and was not intended to undergo liquefaction.

Both the DS and LS layers were prepared under saturated conditions. Before the shaking table test, all sand layers were fully saturated to ensure undrained conditions during dynamic loading. The required volume of water was calculated based on the void ratio and total volume of each sand layer, corresponding to the target relative densities of dense sand (DS), medium sand (MS), and loose sand (LS). The sand was placed dry at the predetermined density and then saturated in stages to achieve uniform saturation and maintain model stability. Water was gradually added from the top at the downstream end, which was leveled over 20 cm to prevent premature slope failure and minimize boundary effects. The required water volume was calculated from the total sand volume and void ratio of each layer. This stepwise saturation ensured full saturation without disturbing the soil structure or altering particle arrangement.

To facilitate sand placement and avoid segregation, a 2 mm sieve (No. 10) was used during filling. Once the sample was prepared, pore pressure transducers were installed, and colored sand markers were placed along one wall. Harmonic shaking was applied with a peak ground acceleration (PGA) of approximately 0.16 g and a frequency of 1.4 Hz for 40 seconds.

3.4 Data Analysis

The analysis focused on two primary parameters: the pore water pressure ratio (Ru = $\Delta u/\sigma'v$) and displacement. The Ru ratio was used to determine the time required to reach full liquefaction (Ru ≈ 1.0), while displacement was evaluated to measure the magnitude of ground movement due to liquefaction. Comparisons were made between capped and uncapped models to assess the role of the capping layer in enhancing or mitigating the potential for flow liquefaction. The Pore Pressure Transducer (PPT) used in this study had an accuracy of ±5% based on calibration. Although error bars are not shown, this uncertainty was accounted for ensure reliable interpretation of the results.

4. RESULT AND DISCUSSION

4.1 Development of Pore Water Pressure

The development of the pore water pressure ratio (Ru) in the model without a capping layer is shown in Fig. 7. The graph illustrates different Ru responses at the three measurement points. Sensor Ru 2, located within the Loose Sand (LS) layer along the centerline, exhibited the most significant increase. Its value rose sharply from the onset of shaking, reaching a peak close to 1.0 at around 37 seconds, coinciding with the end of shaking. After shaking ceased, Ru gradually decreased but stabilized within the range of 0.6–0.7 for an extended period, indicating partial dissipation of excess pore water pressure and a corresponding recovery of effective stress, suggesting, the soil retained only partial shear strength.

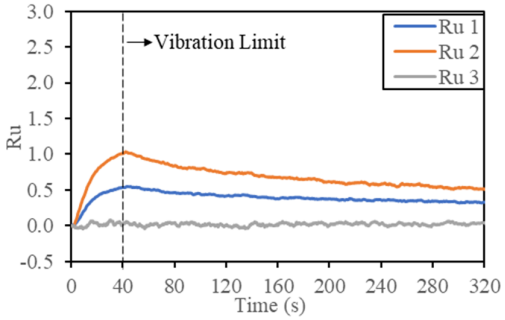

Fig. 7 Ru vs. Time for the Uncapped Model

Although Ru 1 and Ru 2 were both located in the LS layer, the recorded values differed due to their

relative positions and possible drainage pathways. Ru 2 was higher than Ru 1 because its central location favored greater accumulation of pore pressure, while Ru1, positioned closer to the downstream side, allowed more dissipation.

The Medium Sand (MS) layer was placed above the LS, with sensor Ru 3 located at the LS–MS interface. Since the LS layer was saturated and of low relative density, it tended to contract under dynamic loading, generating excess pore pressure. The Ru 3 value remained near zero, indicating that excess pore pressure was confined to the LS zone. Thus, liquefaction was localized at depth, without transmitting to upper layers. This highlights the significance of vertical stratification in determining the depth of the damage zone.

The development of Ru in the capped model is shown in Fig. 8. In this configuration, Ru values increased more rapidly compared to the model without a capping layer model, reaching 1.0 within approximately 11 seconds after shaking began at Ru 1 and Ru 2, while Ru 3 reached the same threshold even earlier, at around 6.8 seconds. This observation suggests that the capping layer accelerated the occurrence of liquefaction in the loose sand layer.

In the capped model, pore pressure not only rose more quickly but also persisted for a longer duration, even after shaking ceased, as observed at Ru3. This phenomenon indicates that the low-permeability silt capping layer acted as a barrier to pore water dissipation, promoting the formation of a water film beneath it. These findings are consistent with previous studies [31,32,33], which suggested that capping layers enhance the likelihood of water film development, subsequently creating a shear plane with nearly zero shear strength.

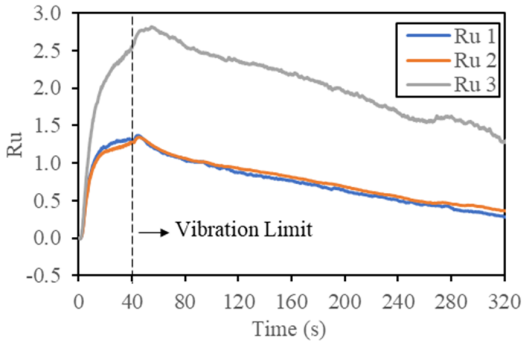

Fig. 8 Ru vs. Time for the Capping Layer

4.2 Displacement

Figure 9 presents the results of displacement measurements conducted after the seismic loading had ceased. The measurements were taken at several points along one side of the sample box. The displacement observed in the model without a capping layer was relatively small, with a maximum displacement not exceeding 0.89 cm, indicating that the system remained in a relatively stable condition.

This displacement was generally concentrated in the upper layers and did not extend across the entire cross-section. This indicates that although soil weakening occurred, the resulting lateral displacement remained limited. As shown in Fig. 7, the Ru values reveal that although Ru 2 temporarily exceeded 1 (indicating liquefaction in the middle layer), the Ru 1 value remained below 1. Consequently, the downstream section of the sample box still functioned as a resisting element, preventing large-scale lateral displacement despite the presence of localized liquefaction.

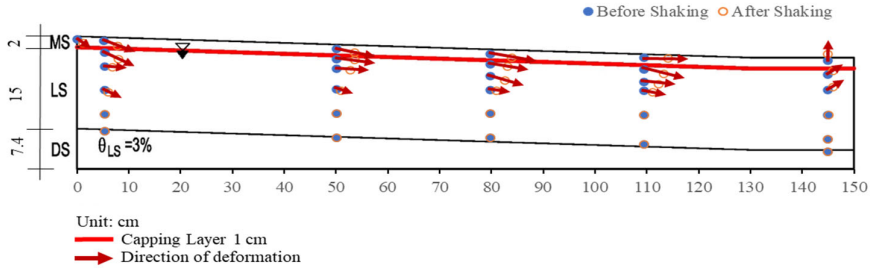

Fig. 9 Lateral Displacement in the Model Without a Capping Layer

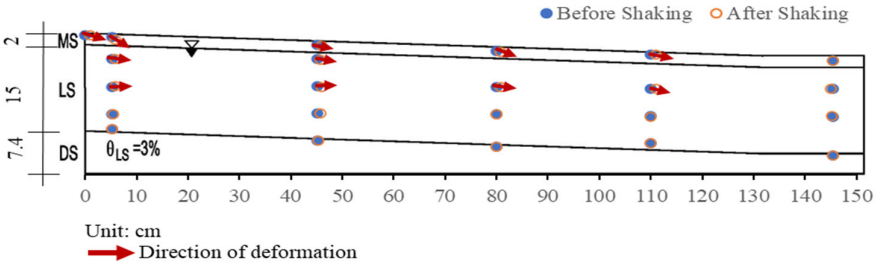

Fig.10 Lateral Displacement in the Model with a Capping Layer

The displacement that occurred was larger and more uniformly distributed along the model. In the model with a capping layer, Ru values increased significantly at all measurement points, reaching as high as 2.8 at PPT 1. This condition indicates that not only the middle layer but also the lower layer had undergone liquefaction. The overall loss of effective stress was the factor that triggered much greater and more uniform displacement. In other words, the magnitude of displacement in the capped model produced a broader liquefied condition compared to the uncapped model. This finding demonstrates that the presence of a capping layer contributes to larger displacement due to the overall weakening mechanism within the soil mass. As also seen in Fig. 10, upward movement took place at the downstream end of the soil model, suggesting a bulging of the near-surface soil layer at this end portion of the soil model. This deformation clearly indicates the occurrence of flow liquefaction in the soil model. It should be noted that the use of a rigid acrylic box in the experiment may have caused partial reflection of seismic waves along the boundaries, potentially influencing the measured pore-water pressure near the walls. To minimize such boundary effects, the downstream portion of the model was constructed flat over a length of 20 cm. This flat section served as a buffer zone to reduce wave reflection and helped maintain a more uniform pore pressure distribution during shaking.

These results are consistent with previous studies. According to Rohit et al. (2021), a low-permeability capping layer can hinder the dissipation of excess pore water pressure, thereby accelerating the onset of liquefaction and maintaining its condition for a longer duration. The accumulation of pore water pressure beneath the capping layer is what causes the loss of effective stress in the underlying layer. Furthermore, Gajan and Kutter (2008) demonstrated that soil layer thickness and density strongly influence deformation behavior, including both settlement and lateral spreading [34]. This is consistent with the present experimental findings, in which the combination of a capping layer and saturated loose sand produced substantially greater deformation compared to the uncapped condition.

4.3 Comparison with Field Conditions

The laboratory findings are consistent with field observations during the 2018 Palu earthquake. Ground flow in Petobo, Balaroa, and Jono Oge occurred on very gentle slopes (2–5%), which would not normally trigger conventional landslides. Geotechnical investigations confirmed the presence of low-permeability layers overlying water-saturated loose sand. Such conditions strongly facilitated water film formation, as demonstrated in this study. Hence, the experimental results provide supporting evidence for the long-distance ground flow mechanism described by Kokusho et al. (2025). Although the shaking table tests in this study used a relatively small PGA of 0.16 g, stronger motions (0.3–0.4 g) are expected to accelerate pore-pressure buildup, prolong its dissipation, and increase lateral deformation. Similar trends reported by Okamura (2022) and Kokusho (2020) indicate that higher PGA levels enhance pore pressure generation and soil mobility during liquefaction.

4.4 Implications for Liquefaction Hazard Evaluation

The results of this study underscore the critical importance of considering soil stratification in liquefaction hazard assessments. While loose sand is inherently susceptible to liquefaction, the presence of a thin capping layer above it significantly increases the hazard — not only by accelerating pore pressure build-up but also by delaying its dissipation. This condition produces much larger lateral displacements compared to uncapped sand. Therefore, liquefaction hazard evaluations should not rely solely on sand properties but must also account for the interactions between layers within the soil stratigraphy.

The experimental method provides valuable insight into pore-pressure development in stratified sand under dynamic loading, though some limitations exist. The small-scale acrylic box may have caused wave reflections and limit deformation, while PPTs record only local responses. The shaking table input was also smaller than that of actual earthquake motions. Nevertheless, the results effectively demonstrate the influence of a low-permeability capping layer on flow liquefaction.

5. CONCLUSION

The experimental results clearly demonstrate that a low-permeability capping layer intensifies both pore-pressure buildup and lateral displacement under seismic loading. Compared with the uncapped model, which exhibited limited deformation, the capped model experienced widespread liquefaction extending into deeper layers, confirming the critical role of stratification in triggering flow-type ground failure. These findings provide valuable insight into real-world liquefaction cases such as the 2018 Palu earthquake, emphasizing that capping layers can significantly exacerbate flow movement even on gentle slopes. Future research should explore the influence of layer thickness and permeability variations to enhance hazard prediction and mitigation strategies, particularly for regions with similar geological settings where the presence of fine-grained layers may further aggravate seismic-induced deformation and increase overall ground failure risk.

6. ACKNOWLEDGMENTS

The authors would like to express their gratitude to BIMA, the Ministry of Education, Culture, Research and Technology for financial support through the Fundamental Research Scheme (Contract No. 032/C3/DT.05.00/PL/2025. Appreciation is also extended to the Soil Testing Laboratory, Department of Civil Engineering, Politeknik Negeri Jakarta, for providing facilities and technical assistance during the implementation of this study.

7. REFERENCES

[1] Ishihara K., "Liquefaction and flow failure during earthquakes," Géotechnique, 1993, doi: 10.1680/geot.1993.43.3.351.

[2] Kramer S.L, Bolton Seed H., and Member H., "Initiation Of Soil Liquefaction Under Static Loading Conditions."

[3] Mason B., Hutabarat D., and Prakoso W., "Geotechnical Reconnaissance: The 28 September 2018 M7.5 Palu-Donggala, Indonesia Earthquake PacTrans-SSI Bridge Project View project Aceh-Pidie Mw 6.5 Earthquake Aftershock 2016 Monitoring View project," Report of Geotechnical Extreme Events Reconnaissance, The Geotechnical Extreme Events Reconnaissance (GEER) Association, no. April, pp. 1–86, 2019, [Online]. Available: https://www.researchgate.net/publication/332221717

[4] Tohari A., Muttaqien I., and Syifa R.W., "Understanding of flow liquefaction phenomena in Palu City from shear wave velocity profiles," E3S Web of Conferences, vol. 340, no. September 2018, pp. 4–9, 2022, doi: 10.1051/e3sconf/202234001011.

[5] Tohari A., Wardhana D.D., Hanif M., and Koizumi K., "Understanding of subsurface conditions controlling flow liquefaction occurrence during the 2018 Palu earthquake based on resistivity profiles," E3S Web of Conferences, vol. 331, pp. 4–8, 2021, doi: 10.1051/e3sconf/202133103002.

[6] Tohari A., Soebowo E., Wibawa S., Hermawan K., and Saputra O.F., "Liquefaction potential analysis for Palu City based on CPT method," IOP Conf Ser Earth Environ Sci, vol. 1173, no. 1, 2023, doi: 10.1088/1755-1315/1173/1/012030.

[7] Rohit D. et al., "Forensic investigation of flowslides triggered by the 2018 Sulawesi earthquake," Prog Earth Planet Sci, vol. 8, no. 1, Dec. 2021, doi: 10.1186/s40645-021-00452-5.

[8] Jalil A., Fathani T.F., Satyarno I., and Wilopo W., "Liquefaction in Palu: the cause of massive mudflows," Geoenvironmental Disasters, vol. 8, no. 1, 2021, doi: 10.1186/s40677-021-00194-y.

[9] Upomo T.C., Chang M., Kusumawardani R., Prayitno G.A., Huang R.C., and Fansuri M.H., "An Overview Study of Flowslide Liquefaction in Petobo, Palu, Indonesia," IOP Conf Ser Earth Environ Sci, vol. 1203, no. 1, 2023, doi: 10.1088/1755-1315/1203/1/012007.

[10] Kusumawardani R., Chang M., Upomo T.C., Huang R.C., Fansuri M.H., and Prayitno G.A., "Understanding of Petobo liquefaction flowslide by 2018.09.28 Palu-Donggala Indonesia earthquake based on site reconnaissance," Landslides, vol. 18, no. 9, pp. 3163–3182, Sep. 2021, doi: 10.1007/s10346-021-01700-x.

[11] Kiyota T., Furuichi H., Hidayat R.F., Tada N., and Nawir H., "Overview of long-distance flow-slide caused by the 2018 Sulawesi earthquake, Indonesia," Soils and Foundations, vol. 60, no. 3, pp. 722–735, Jun. 2020, doi: 10.1016/j.sandf.2020.03.015.

[12] Tanjung M.I., Irsyam M., Sahadewa A., Iai S., Tobita T., and Nawir H., "Overview of Flowslide in Petobo during liquefaction of the 2018 Palu Earthquake," Soil Dynamics and Earthquake Engineering, vol. 173, Oct. 2023, doi: 10.1016/j.soildyn.2023.108110.

[13] Okamura M., "Factors Affecting Liquefaction Resistance and Assessment by Pore Pressure Model," in Geotechnical, Geological and Earthquake Engineering, vol. 52, Springer Science and Business Media B.V., 2022, pp. 120–139. doi: 10.1007/978-3-031-11898-2_7.

[14] Okamura M., Ono K., Arsyad A., Minaka U.S., and Nurdin S., "Large-scale flowslide in Sibalaya caused by the 2018 Sulawesi earthquake," Soils and Foundations, vol. 60, no. 4, pp. 1050–1063, Aug. 2020, doi: 10.1016/j.sandf.2020.03.016.

[15] Kokusho T., "Earthquake-induced flow liquefaction in fines-containing sands under initial shear stress by lab tests and its implication in case histories," Soil Dynamics and Earthquake Engineering, vol. 130, Mar. 2020, doi: 10.1016/j.soildyn.2019.105984.

[16] Robertson P.K., "Evaluation of flow liquefaction and liquefied strength using the cone penetration test: an update," 2022, Canadian Science Publishing. doi: 10.1139/cgj-2020-0657.

[17] Cetin K.O. et al., "Examination of differences between three SPT-based seismic soil liquefaction triggering relationships," Soil Dynamics and Earthquake Engineering, vol. 113, pp. 75–86, 2018.

[18] Kayen R. et al., "Shear-wave velocity–based probabilistic and deterministic assessment of seismic soil liquefaction potential," Journal of Geotechnical and Geoenvironmental Engineering, vol. 139, no. 3, pp. 407–419, 2013.

[19] Kutter B.L., Manzari M.T., and Zeghal M., "Model Tests and Numerical Simulations of Liquefaction and Lateral Spreading."

[20] Ni X., Ye B., Ye G., and Zhang F., "Unique determination of cyclic instability state in flow liquefaction of sand," Marine Georesources and Geotechnology, pp. 1–9, 2020, doi: 10.1080/1064119X.2020.1791289.

[21] Nie Z, Chi S., and Gong S., "Numerical Modeling of Cyclic Triaxial Experiments for Granular Soil," International Journal of Geomechanics, vol. 17, no. 6, Jun. 2017, doi: 10.1061/(asce)gm.1943-5622.0000832.

[22] Miao F., Wu Y., Török A., Li L., and Xue Y., "Centrifugal model test on a riverine landslide in the Three Gorges Reservoir induced by rainfall and water level fluctuation," Geoscience Frontiers, vol. 13, no. 3, May 2022, doi: 10.1016/j.gsf.2022.101378.

[23] Qiu Z. and Elgamal A., "LEAP-ASIA-2019 Centrifuge Test Simulations of Liquefiable Sloping Ground," in Model Tests and Numerical Simulations of Liquefaction and Lateral Spreading II, Springer International Publishing, 2024, pp. 369–385. doi: 10.1007/978-3-031-48821-4_17.

[24] Kokusho T., "Current state of research on flow failure considering void redistribution in liquefied deposits," Soil Dynamics and Earthquake Engineering, vol. 23, no. 7, pp. 585–603, 2003, doi: 10.1016/S0267-7261(03)00067-8.

[25] Rohit D. et al., "Simulation of water film formation during the 2018 Sulawesi earthquake, Indonesia," Proceedings of the Institution of Civil Engineers: Forensic Engineering, vol. 176, no. 4, pp. 119–133, May 2022, doi: 10.1680/jfoen.21.00024.

[26] Tokida I.T.K., Matsumoto H., Azuma T., "Simplified procedure to estimate lateral ground flow by soil liquefaction," Transactions on the Built Environment, vol. 3, 1995.

[27] Hamada M, Towhata I., Yasuda S., and Isoyama R., "Study on permanent ground displacement induced by seismic liquefaction," Comput Geotech, vol. 4, no. 4, pp. 197–220, Jan. 1987, doi: 10.1016/0266-352X(87)90001-2.

[28] Tokida K., Matsumoto H., Azuma T., and Towhata I., "Simplified procedure to estimate lateral ground flow by soil liquefaction," 1993. [Online]. Available: www.witpress.com,

[29] Toyota H., Towhata I., Imamura S.I. and Kudo K.I., "Shaking table tests on flow dynamics in liquefied slope," Soils and Foundations, vol. 44, no. 5, pp. 67–84, 2004, doi: 10.3208/sandf.44.5_67.

[30] Tsuchida H., "Prediction and Countermeasure against Liquefaction in Sand Deposits," 1970.

[31] Kokusho T., "NII-Electronic Library Service Mechanism for Water Film Generation and Lateral Flow in Liquefied Sand Layer," Japanese Geotechnical Society, 2000.

[32] Kokusho T., Sawada T., Hazarika H., and Isobe Y., "Long-distance flow mechanism of gentle slopes under seepage due to liquefaction-induced water film during 2018 Sulawesi earthquake, Indonesia," Soils and Foundations, vol. 65, no. 3, Jun. 2025, doi: 10.1016/j.sandf.2025.101611.

[33] Rohit D., Pasha S.M.K., Hazarika H., Kokusho T., Nurdin S., "Influence of Low Permeability Capping Layers on Liquefaction Induced Failure in Stratified Ground," in Proceedings of the Indian Geotechnical Conference 2019, Springer Nature, May 2021.

[34] Kutter B.L., Gajan S., Manda K.K., and Balakrishnan A., "Effects of Layer Thickness and Density on Settlement and Lateral Spreading," Journal of Geotechnical and Geoenvironmental Engineering, vol. 130, no. 6, pp. 603–614, Jun. 2004, doi: 10.1061/(asce)1090-0241(2004)130:6(603).